Near-Critical NaCl–H$_2$O: An Equation of State and Discussion of Anomalous Properties[1]

Kenneth S. Pitzer[2] and John C. Tanger IV[2]

The system NaCl–H$_2$O near the critical point of pure water shows not only the remarkable properties of any two-component system near the critical point of one component but also an anomalous curvature of the T–x and P–x projections of the critical line in the range below mole fraction 0.0005. An equation of state is presented which is based on the Haar–Gallagher–Kell equation for pure water with a few terms involving the mole fraction of NaCl together with the temperature and density. Parameters in this equation were selected which yield a good representation of the entire vapor-liquid coexistence surface from 250 to 600°C and from the three-phase pressure to the critical pressure (or to the vapor pressure of pure water below its T_c). Derivatives of this equation yield densities, enthalpies, and heat capacities which are compared with experimental data. Also, the properties calculated for the vapor near the three-phase line are compared with those predicted by the successive hydration model previously developed for NaCl in steam in equilibrium with solid NaCl. Other related topics are discussed, including the anomalous features noted above.

KEY WORDS: coexistence surface; critical region; mixtures (binary); sodium chloride; water.

1. INTRODUCTION

A two-component fluid shows some remarkable properties near the critical point of one component. The pertinent theory on a classical basis has been given by several investigators. Rozen [1] found good agreement on this basis for the P–x and T–x projections of the critical line for SF$_6$–CO$_2$. For the very interesting and practically important system NaCl–H$_2$O, however, the P–x and T–x critical lines show such rapid changes in slope near the

critical point of pure H_2O that a quantitative treatment on a similar basis was frustrated [2]. It was then shown that such a quantitative treatment could be given if it was based on a "classical" critical point for pure water instead of the true critical point [3].

While pure H_2O shows nonclassical behavior near its critical point with a coexistence curve consistent with a critical exponent $\beta \cong 0.325$, a solution of NaCl with as small a mole fraction as 0.0009 shows classical behavior with $\beta = \frac{1}{2}$ [4]. Thus, it appears that the long-range interparticle forces of the NaCl suppress the extra, nonclassical fluctuation effects of pure H_2O.

In brief reports recently published, a simple equation of state was proposed and applied [3] to phase-equilibrium data very close to the critical line and extending to 380°C [4]. We now present an improved equation which represents the entire vapor–liquid equilibrium surface for $NaCl–H_2O$ from the three-phase pressure to the critical pressure and from below the critical temperature of water to 600°C (873 K). This equation is based on that of Haar et al [5] for pure H_2O and connects to the true critical point of H_2O. The anomalous curvature of the critical line for $NaCl–H_2O$ arises from the nonclassical, near-critical properties of H_2O as expressed in the Haar equation and their rapid disappearance in the solution. While other types of data were not used in fitting this equation, the pressure and temperature derivatives yield reasonably good values for other properties including the apparent molar heat capacity for conditions near the critical line. This paper includes a description of this equation and comparisons of calculated curves with certain measured properties, primarily in the region near the critical point of pure H_2O. In another paper, comparisons are presented for a wider range of temperature and for properties of geological interest [6].

2. SELECTION OF THE EQUATION OF STATE

The basic concept of the equation is an expansion around the critical point of water. For the properties of pure water, however, we take the complete equation of Haar, Gallagher, and Kell (HGK) [5], which is valid over a very wide range of pressure, volume, and temperature. The effect of NaCl is expressed by a very small number of temperature-dependent terms in increasing powers of the amount of salt added and of the density difference from the critical density of H_2O. It is convenient to take as a basis 1 mol of H_2O and y mol of NaCl; thus, y is the mole ratio and the mole fraction $x = y/(1 + y)$. We use the density of water in the system, $\rho(H_2O) = \rho(\text{solution})(1 - \text{wt. fraction NaCl})$, and define the reduced

density $d = \rho(H_2O)/\rho_c(H_2O)$, with $\rho_c(H_2O)$ the critical density of pure water. Then one writes for the pressure

$$P = P_{H_2O}(T, d) + y[b_{10} + b_{11}(d-1) + \cdots] + y^2[b_{20} + \cdots] + \cdots \quad (1)$$

Here P_{H_2O} is the pressure of pure H$_2$O calculated from the HGK equation for T and d.

Much of the literature [2] on two-component fluid properties close to the critical point of one component uses an expansion of the molar Helmholtz energy:

$$a = a^c + a_v^c(\delta V) + a_T^c(\delta T) + a_x^c x + a_{vx}^c(\delta V)x + \cdots$$
$$+ a_{vvT}^c(\delta V)^2 (\delta T)/2 + a_{vvx}^c(\delta V)^2 x/2 + \cdots + RTx \ln x \quad (2)$$

where the subscripts indicate differentiation by that variable and the superscript c indicates evaluation at the critical point of the solvent. In these terms the initial slope of the two-component critical line is given by

$$(dT/dx)_{CRL}^c = [(a_{vx}^c)^2/RT_c - a_{vvx}^c]/a_{vvT}^c \quad (3)$$

In terms of Eq. (1), b_{10} is $-a_{vx}^c$ and b_{11} is $-a_{vvx}^c/\rho_c(H_2O)$, while a_{vvT}^c is given by differentiation of P_{H_2O}. Thus, the two terms in b_{10} and b_{11} are clearly required to express even the initial slope of the critical line. To our surprise, we were able to obtain quite good agreement with the vapor-liquid coexistence surface over a wide range of temperature and pressure with just the one additional term $y^2 b_{20}$ shown explicitly in Eq. (1). Each of the b_{ij} quantities is temperature dependent, although their changes near $T_c(H_2O)$ are small.

The expression for the pressure can be integrated to yield the density-dependent terms of the Helmholtz energy; then density-independent terms are added. An ideal mixing term (on the undissociated basis) and a temperature-dependent term proportional to y are chosen for the latter, although a more complex function of T and y could have been selected. One then obtains

$$A/n_{H_2O} = a_{H_2O}(T, d) + v_c y[-b_{10}/d + b_{11}(\ln d + 1/d)] - v_c y^2 b_{20}/d$$
$$+ RT[y \ln y - (1 + y) \ln(1 + y)] + y g_{NaCl}^*(T) \quad (4)$$

with v_c the critical volume of pure water. Here the basis is 1 mol of water and the ideal mixing term has been transformed from the familiar form in x to the corresponding form for the mole ratio y. The quantity $g_{NaCl}^*(T)$ can be evaluated by comparison of the chemical potential of NaCl.

Addition of the PV term to Eq. (4) yields the Gibbs energy, when transformed to the basis of 1 mol of solution, it becomes

$$G/(n_{H_2O} + n_{NaCl}) = (1 - x)g_{H_2O}(T, d) + RT[x \ln x + (1 - x) \ln(1 - x)]$$
$$+ xv_cb_{11}(1 + \ln d) + xg_{NaCl}^*(T) \qquad (5)$$

One may now calculate the compositions of coexisting vapor and liquid phases by first calculating the density as a function of x (or y) at constant T and P from Eq. (1) (by iteration). Substitution of d into Eq. (5) then gives the molar Gibbs energy as a function of x, and the double tangent locates the equilibrium compositions. By trial and adjustment, values of b_{10}, b_{11}, and b_{20} were found which yielded reasonable agreement with the coexistence surface; this process is described more fully below.

Other thermodynamic properties are obtained from appropriate derivatives; a few examples are

$$H/n_{H_2O} = h_{H_2O}(T, d) + yv_c[(T/d)(db_{10}/dT + ydb_{20}/dt)$$
$$- T(db_{11}/dT)(\ln d + 1/d) + b_{11}(1 + \ln d)] + yh_{NaCl}^*(T) \quad (6)$$

$$C_V/n_{H_2O} = c_{v,H_2O}(T, d) + yv_c(T/d)[(d^2b_{10}/dT^2) + y(d^2b_{20}/dT^2)$$
$$- (d \ln d + 1)(d^2b_{11}/dT^2)] + yc_{NaCl}^*(T) \qquad (7)$$

$$(\partial P/\partial T)_d = (\partial P_{H_2O}/\partial T)_d + y[(db_{10}/dT) + (d - 1)(db_{11}/dT)]$$
$$+ y^2(db_{20}/dT) \qquad (8)$$

Apparent molar quantities can be calculated from the appropriate differences; the apparent molar volume, for example, is

$$\phi_V = (V_S - V_{H_2O})/n_{NaCl} = (v_c/y)(1/d_s - 1/d_o) \qquad (9)$$

In Eq. (9) the symbol d_s refers to the reduced density of water in the solution, while the symbol d_o refers to the reduced density of pure water at the pressure and temperature of the solution. The function $c^*(T)$ is related by the usual temperature derivative to $g^*(T)$. Various quantities can be combined to give other thermodynamic properties, including the heat capacity at constant pressure.

Clearly, the b_{10} and b_{11} terms arise from the hydration of NaCl, the b_{10} for water of critical density, and the b_{11} term for the effect of change from critical density. At zero concentration, the NaCl will be fully dissociated so that this should be the sum of the hydration effects for Na$^+$ and Cl$^-$. We know, however, from the conductance measurements of Quist and Marshall [7] that NaCl in critical H$_2$O is a weak electrolyte and that it is largely associated to ion pairs at the concentrations we consider. Thus, the

b_{10} term actually represents the hydration effect of a distribution of ion pairs together with some separated Na$^+$, Cl$^-$ ions and the b_{11} term gives the combined effect of a change in density of water on the hydration process and on the degree of association of the NaCl. The $y^2 b_{20}$ term, which is included, becomes important only for quite concentrated liquids where various binary solute interactions will be present.

3. EVALUATION OF PARAMETERS; THE VAPOR-LIQUID COEXISTENCE SURFACE

The three parameters b_{10}, b_{11}, and b_{20} were first evaluated from the vapor–liquid coexistence curves at a series of temperatures from 250 to 600°C (523–873 K). Figure 1 shows that the equation represents very well the remarkable changes from 373 to 440°C near the critical point of pure water [8–10]. Figures 2 and 3 show that good agreement is also obtained for the liquid phase down to 250°C [11–15] and for both phases up to 500°C [16–18]. At temperatures below 373°C the vapor (steam) phase contains very little NaCl and the composition is difficult to measure. We
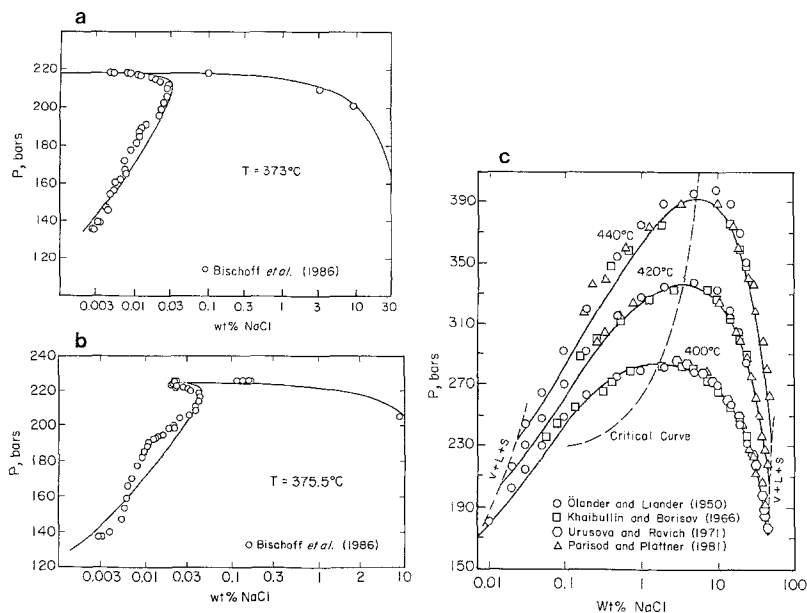

Fig. 1.   The phase diagram for NaCl–H$_2$O (a) at 373°C, just below T_c; (b) at 375.5°C, just above T_c; and (c) at 400, 420, and 440°C. The curves are calculated from Eqs. (1) and (5), while the experimental values are from Bischoff et al. [8], Olander and Liander [9], Khaibullin and Borisov [10], Urusova and Ravich [11], and Parisod and Plattner [12]. One bar = 0.1 MPa.
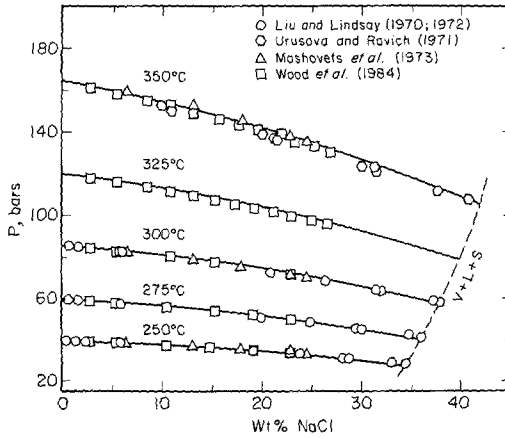
Fig. 2. Liquid phase compositions in equilibrium with the vapor at below-critical temperatures. The curves are calculated from Eqs. (1) and (5). Experimental values are from Liu and Lindsay [13], Urusova and Ravich [11], Mashovets et al. [14], and Wood et al. [15].

accepted the measurements of Bischoff et al. [8] for the vapor in equilibrium with solid and liquid and these are fitted accurately.

In fitting parameters, primary emphasis was placed on the vapor and liquid compositions at the three-phase pressure (vapor + liquid + solid equilibrium) and on the critical pressure. Finally, temperature-dependent equations for each of the three parameters were fitted as follows:
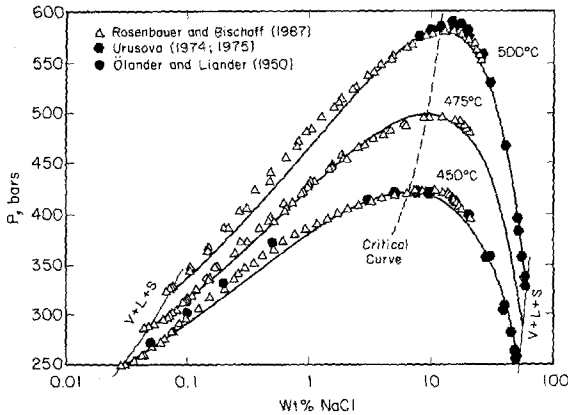
Fig. 3. Vapor and liquid compositions along the coexistence curves for 450, 475, and 500°C. The curves are calculated from Eqs. (1) and (5). Experimental values are from Olander and Liander [9], Urusova [16, 17], and Rosenbauer and Bischoff [18].

$$b_{10} = -29,984.4 + 19.0285T + 6.65541 \times 10^{12}/T^3 - 1.20069 \times 10^{18}/T^5 \quad (10)$$

$$b_{11} = 3928.3 - 10.5947T - 6.0751 \times 10^{38}/T^{13} \quad (11)$$

$$b_{20} = 14,121.9 - 27.0731T - 2.57142 \times 10^{23}/T^7 \quad (12)$$

The units are bars with T in K (1 bar $= 0.1$ MPa). Further details concerning this fitting procedure are given elsewhere [6].

4. OTHER PROPERTIES

4.1. Heat Capacity

Comparisons of heat capacities involve the initially unknown function $c_{NaCl}^*(T)$ which appears in Eq. (7). In the range above 320°C, a zero value of c_{NaCl}^* gave acceptable agreement with measurements of White et al. [21]. At lower temperatures, however, there were large discrepancies with data from references [19] and [20], which is not surprising since the calculations involve second derivatives of the empirical Eqs. (10)–(12) for the parameters b_{10}, b_{11}, and b_{20} near the lower end of their range of validity. The following expression for c_{NaCl}^* gives good agreement:

$$c_{NaCl}^*/R = -2.3 \times 10^{46}T^{-16} \quad (13)$$

with T in K.

Figure 4 compares our caluclated curve for the apparent molar heat capacity of NaCl at the very low molality 0.015 with very recent measurements of White et al. [21] at 321 bars. Our equation yields with remarkable accuracy the extremely large heat capacities, negative near 395°C and positive near 415°C. If our curve were shifted down in temperature by a few degrees, the agreement would be nearly perfect. The agreement shown in Fig. 4 gives some confirmation to our equation in the range above 350°C where there are, to our knowledge, no heat capacity measurements at higher molalities or different pressures.

4.2. Chemical Potentials, Entropy, and Enthalpy

The chemical potentials of H$_2$O and NaCl and various thermal quantities involve either the function $g_{NaCl}^*(T)$ or its temperature derivatives. We may now integrate Eq. (13) to obtain the following expressions for the entropy, enthalpy, and free energy:

$$s^*(T)/R = 1.47 \times 10^{45}T^{-16} + s_0^*/R \quad (14)$$

$$[h^*(T) - H_{298}^0]/R = 1.57 \times 10^{45}T^{-15} + (h_0^* - H_{298}^0)/R \quad (15)$$

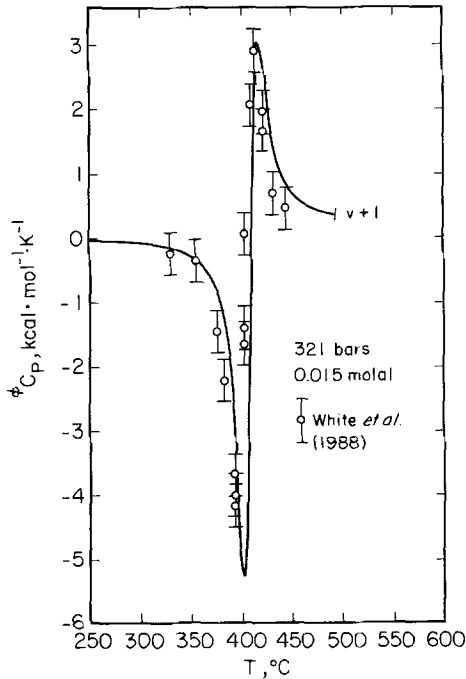$$[g^*(T) - H_{298}^0]/RT = 1.0 \times 10^{44}T^{-16} + (h_0^* - H_{298}^0)/RT - s_0^*/R \quad (16)$$

Fig. 4. Apparent molar heat capacity of a 0.015
molal solution at 321 bars. The vertical bars
represent our estimated uncertainties for the
experimental values of White et al. [21]; the curve
is calculated from the equations of this research.
One kilocalorie = 4.184 kJ.

Since there is no natural zero of enthalpy, the difference from a standard
state value is shown.

The two parameters in Eq. (16), $(h_0^* - H_{298}^0)/R$ and s_0^*/R, can be
evaluated by considering the equilibrium of aqueous NaCl with solid NaCl
over a range of temperature. This equilibrium is of geochemical interest
and is discussed in detail elsewhere [6]. We report here just the values
selected: $(h_0^* - H_{298}^0)/R = 1900$ K and $s_0^*/R = 10.0$, where H_{298}^0 is the
enthalpy of solid NaCl at 298 K and s_0^* is a molar entropy on an absolute
basis. Comparison was then made with enthalpies and entropies for 3.2%
NaCl from Bischoff and Rosenbauer [22]; the agreement was good.

In general, extrapolation of the present equation to zero-mole fraction
NaCl will not yield reliable properties for NaCl in its standard state at
infinite dilution. At low densities where the NaCl is largely ion paired, the
extrapolated values will be approximately correct for the ion-paired stan-

dard state. But this equation includes no provision for dissociation; hence, it cannot yield valid results for the ionized standard state. This situation is considered more fully elsewhere [6].

4.3. Vapor Near the Three-Phase Pressure

The concentration of NaCl is very low in the vapor at pressures near the three-phase line and temperatures below 400°C. Experimental measurements are difficult and the reported values vary widely. We adopted the composition curve of Bischoff et al. [8] for the three-phase pressure as did Pitzer and Pabalan [23] in developing an equation of a very different type for NaCl in steam in equilibrium with solid NaCl. Thus the two equations give the same composition at the three-phase pressure. It is of considerable interest to compare the predictions of the two equations at pressures below and above the three-phase pressure. This is shown in Fig. 5 for 350°C. The curve represents the calculated composition from the present equation above the three-phase pressure and from the Pitzer–Pabalan equation below that pressure. The X's show the metastable
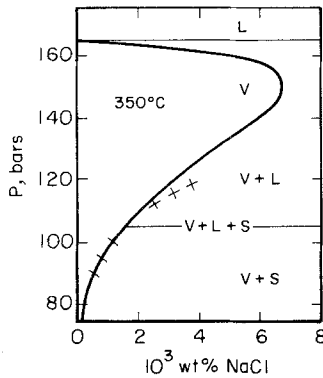

Fig. 5. Vapor composition in equilibrium with the solid below the three-phase pressure and in equilibrium with the liquid above that pressure. The curves are calculated, respectively, by the equation of Pitzer and Pabalan [23] and the present equation. The X's represent calculated metastable extensions of one equation into the pressure range of the other.

extensions for each equation into the other pressure range. It is clear that the pressure dependencies of the two equations agree quite satisfactorily. Thus we believe that considerable confidence can be placed in the predictions of the present equation for the vapor composition in this range where experimental values are sparse and uncertain.

5. VOLUMETRIC PROPERTIES AT NEAR-CRITICAL TEMPERATURES

Figures 6 and 7 show the very interesting volumetric behavior of isotherms near the critical temperature. In Fig. 6 the dashed-dotted lines show the tie lines connecting vapor and liquid at equilibrium, while the dashed lines are tangent to the isotherms at their critical points and extrapolate at zero mole fraction to the partial molar volume of water. One notes that, for conditions along the critical line, this partial molar volume of H_2O increases and finally diverges to plus infinity in the limit of zero NaCl.
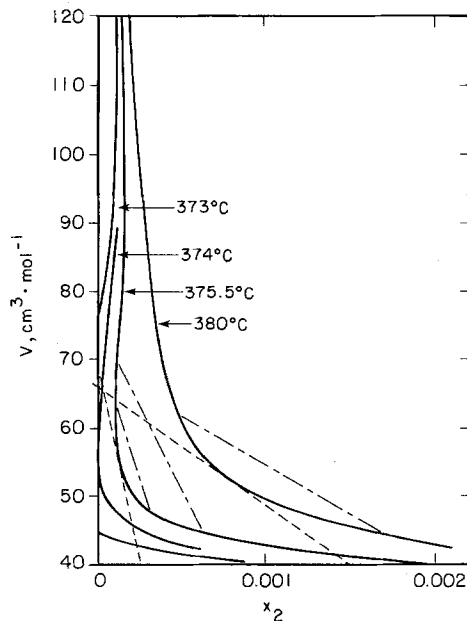
Fig. 6. Volumetric behavior of isotherms from 373 to 380°C. The dashed tangents at the critical compositions extrapolate at $x_2 = 0$ to the partial molar volume of H_2O. The tie lines are dashed-dotted.
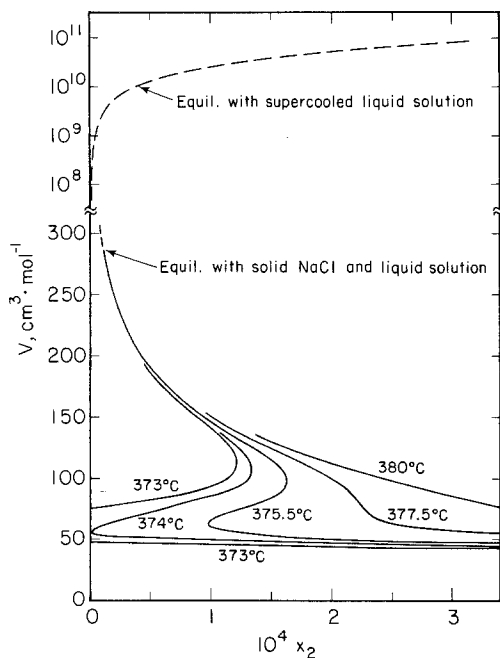
Fig. 7. The volumetric behavior over a very wide range of volume. The dashed portion of the curve is for equilibrium with supercooled liquid.

Figure 7 shows the behavior over a wider range of volume. The near-critical isotherms show a maximum in the NaCl fraction in the vapor at volumes near $100 \; cm^3 \cdot mol^{-1}$ and a minimum near the critical volume of pure H_2O ($56 \; cm^3 \cdot mol^{-1}$). Only a shoulder remains at 377.5°C, and by 380°C the V–x curve has a simple shape.

The NaCl content of steam drops to a very low level as the volume increases to the three-phase conditions (vapor + liquid + halite). At still larger volumes the vapor is essentially pure steam until the pressure approaches the vapor pressure of pure NaCl, either supercooled liquid or solid.

The present equation provides a basis for convenient calculation of other projections of volumetric properties and of enthalpies and other similar properties of the system NaCl–H₂O. Also, the general pattern of the behavior of near-critical NaCl–H₂O should be typical of systems with one nonvolatile component. Thus, this equation can be used for qualitative or semiquantitative calculations for other similar systems.

6. BEHAVIOR VERY NEAR THE CRITICAL POINT OF WATER

Before discussing the effect of very small amounts of NaCl, it is desirable to recognize certain aspects of the HGK equation for pure H_2O. Initially, Haar et al. [24] developed an equation fitting all properties everywhere except for a small region close to the critical point. This can be taken as a "classical" equation of state for H_2O. Then in 1984 they added a three-term function that is significant only very close to the critical point [5]. While the complete equation does not have the correct limiting critical-exponential properties, it represents all experimental data for H_2O quite accurately. Thus, from an empirical viewpoint, the three-term function of 1984 gives the effect of the near-critical, nonclassical fluctuations which lower the critical temperature from the 375.1°C of the 1980 HGK equation to 374.0°C, the true value.

We used both the "classical" (1980) equation and the complete (1984) equation in our calculations. Only at 375.5°C was there a significant difference for the isothermal coexistence curve; this is shown on an expanded scale in Fig. 8. The uncertainties in pressure and temperature measurement, however, are larger than the difference between the two curves. Figure 9 shows the calculated $T–x$ critical lines on the two bases. The classical calculation shows only a small curvature and a finite slope at $x = 0$, in agreement with Eq. (3). The curve based on the complete HGK equation shows a large curvature in the region where the nonclassical fluctuation effect is important. Since a_{vvt}^c is zero on the nonclassical basis, the slope is infinite in the limit at the critical point if the other quantities remain finite.

In view of the experimental uncertainties and the simplicity of our Eq. (1), one should not overemphasize the details at the limit $x \rightarrow 0$. Nevertheless, it seems clear that the anomalous curvature of the critical line
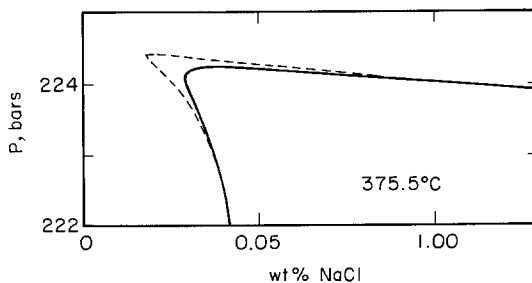
Fig. 8. Coexistence curves for 375.5°C. The solid curve was calculated with the complete HGK equation for H_2O, while the dashed curve was calculated with the "classical" equation of Haar et al. [24].

Fig. 9. The critical line for H$_2$O–NaCl near the critical point of pure water. The solid curve was calculated with the complete HGK equation for H$_2$O, while the dashed curve was calculated with the "classical" equation of Haar et al. [24].
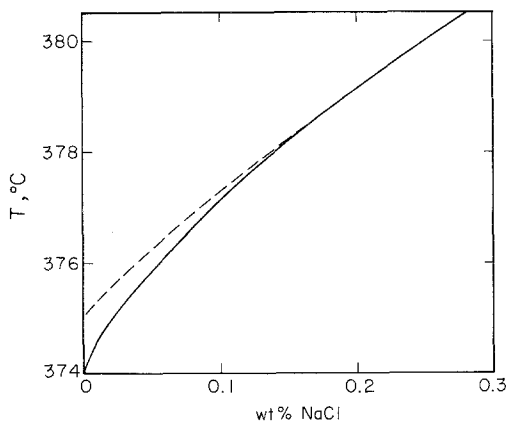
near the critical point of pure water is associated with a rapid decrease in the additional, nonclassical fluctuation effect in pure H$_2$O as a small concentration of ions is added.

7. DISCUSSION

Two different but related types of equations have been used to represent the near-critical properties of NaCl–H$_2$O and related systems. The more detailed type considers the solvation energy, using the Born equation, and the ion-interaction effects. Each term depends strongly on the dielectric constant of water and this introduces striking effects near the critical point. But there are many approximations in the published editions of these theories and, as discussed by White et al. [21], only qualitative agreement has been attained. In the other type of theory, the effect of the solute is expressed by a simple adjustment of the properties of water. Wood and Quint [25] proposed a "corresponding-states" theory, i.e., that the properties of the solution are the same as those of water at the same reduced temperature and pressure. As noted by White *et al.* [21], this theory gives qualitatively correct results for the apparent molar heat capacity of 0.015 mol · kg^{-1} solution at 321 bars (Fig. 4), but the minimum near T_c is not deep enough and the following maximum is much too high. The present theory relates the properties of the solution to those of water at a shifted density but an unchanged temperature. For most properties

there are small additional terms proportional to the amount of NaCl present, but the striking near-critical effects arise from the density shift for the equation of state for H_2O. The success of the present equation recommends it for use for similar systems including those with mixed solutes.

ACKNOWLEDGMENTS

REFERENCES

1. A. M. Rozen, *Russ. J. Phys. Chem.* **50**:837 (1976) (English).
2. J. M. H. Levelt Sengers, C. M. Everhart, G. Morrison, and K. S. Pitzer, *Chem. Eng. Commun.* **47**:315 (1986); R. F. Chang, G. Morrison, and J. M. H. Levelt Sengers, *J. Phys. Chem.* **88**:3389 (1984); J. M. H. Levelt Sengers, *Proc. Int. Conf. Thermodyn. Aqueous Syst. Indust. Appl.*, Warrenton, Va, 1987 (Hemisphere, Washington, D.C., 1988, in press).
3. K. S. Pitzer, *J. Phys. Chem.* **90**:1502 (1986a).
4. K. S. Pitzer, J. L. Bischoff, and R. J. Rosenbauer, *Chem. Phys. Lett.* **134**:60 (1987).
5. L. Haar, J. S. Gallagher, and G. S. Kell, *NBS-NRC Steam Tables* (Hemisphere, Washington, D.C., 1984).
6. J. C. Tanger IV and K. S. Pitzer, *Geochim. Cosmochim. Acta* (in press).
7. A. S. Quist and W. L. Marshall, *J. Phys. Chem.* **72**:684 (1968).
8. J. L. Bischoff, R. J. Rosenbauer, and K. S. Pitzer, *Geochim. Cosmochim. Acta* **50**:1437 (1986).
9. A. Olander and H. Liander, *Acta Chem. Scand.* **4**:1437 (1950).
10. Kh. Khaibullin and N. M. Borisov, *Teplofiz. Vysokikh Temp.* **4**:489 (1966) (in English).
11. M. A. Urusova and M. I. Ravich, *Russ. J. Inorg. Chem.* **16**:1534 (1971).
12. C. J. Parisod and E. Plattner, *J. Chem. Eng. Data* **26**:15 (1981).
13. C. Liu and W. T. Lindsay, Jr., *J. Phys. Chem.* **74**:341 (1970); *J. Solut. Chem.* **1**:45 (1972).
14. V. P. Mashovets, V. I. Zarembo, and M. K. Federov, *J. Appl. Chem. USSR* **46**:684 (1973).
15. S. A. Wood, D. A. Crerar, S. L. Brantley, and M. Borcsik, *Am. J. Sci.* **284**:668 (1984).
16. M. A. Urusova, *Russ. J. Inorg. Chem.* **19**:450 (1974).
17. M. A. Urusova, *Russ. J. Inorg. Chem.* **20**:1717 (1975).
18. R. J. Rosenbauer and J. L. Bischoff, *Geochim. Cosmochim. Acta* **51**:2349 (1987).
19. D. Smith-Magowan and R. H. Wood, *J. Chem. Thermo.* **13**:1047 (1981).
20. J. A. Gates, D. M. Tillett, D. E. White, and R. H. Wood, *J. Chem. Thermo.* **19**:131 (1987).
21. D. E. White, R. H. Wood, and D. R. Biggerstaff, *J. Chem. Thermo.* **20**:159 (1988).
22. J. L. Bischoff and R. J. Rosenbauer, *Am. J. Sci.* **285**:725 (1985).
23. K. S. Pitzer and R. T. Pabalan, *Geochim. Cosmochim. Acta* **50**:1445 (1986).
24. L. Haar, J. S. Gallagher, and G. S. Kell, in *Water and Steam*, J. Straub and K. Scheffler, eds. (Pergamon, Oxford, 1980), p. 69.
25. R. H. Wood and J. R. Quint, *J. Chem. Thermo.* **14**:1069 (1982).